Exergy and sensibility analysis of each individual effect in a kraft multiple effect evaporator

JÉSSICA MOREIRA, BRUNO LACERDA DE OLIVEIRA CAMPOS, ESLY FERREIRA DA COSTA JUNIOR, AND ANDRÉA OLIVEIRA SOUZA DA COSTA

ABSTRACT: The multiple effect evaporator (MEE) is an energy intensive step in the kraft pulping process. The exergetic analysis can be useful for locating irreversibilities in the process and pointing out which equipment is less efficient, and it could also be the object of optimization studies. In the present work, each evaporator of a real kraft system has been individually described using mass balance and thermodynamics principles (the first and the second laws). Real data from a kraft MEE were collected from a Brazilian plant and were used for the estimation of heat transfer coefficients in a nonlinear optimization problem, as well as for the validation of the model. An exergetic analysis was made for each effect individually, which resulted in effects 1A and 1B being the least efficient, and therefore having the greatest potential for improvement. A sensibility analysis was also performed, showing that steam temperature and liquor input flow rate are sensible parameters.

Application: The exergetic analysis results show that it is possible for mill personnel to determine which evaporators have the highest and lowest energy losses in the actual kraft pulp production process.

In a kraft pulp mill process, the cellulose pulp is obtained from wood chips [1-3], and a black liquor is produced, which is a byproduct rich in organic matter. The liquor treatment is a step of great importance in the pulp mill. During this recovery process, feedstock is recovered, steam is produced, and environmental impacts are reduced. The black liquor is concentrated in a multiple effect evaporator (MEE) and is then sent to the recovery boiler, where it is burned to produce steam and to produce the green liquor, which follows to the causticizing section. The steam is also used in the kraft process to generate power [4-6].

The kraft pulping process consumes a high amount of energy, especially due to the evaporation step in which there is significant energy demand for the water vaporization [7-11]. By implementing programs that reduce the required amount of energy, either by improving energy distribution or equipment efficiency, it is possible to maintain a competitive position in the market [12]. Therefore, it is interesting to research promising methodologies and/or technologies capable of improving energetic efficiency.

Mill engineers have traditionally considered only energy analysis to establish the most efficient operating conditions and have ignored the irreversibilities of the system. However, the exergetic analysis can provide another point of view about the energetic efficiency of the industrial system. The exergetic analysis complements the energetic analysis and has many uses, such as to locate irreversibilities in the process; to estimate the minimum required energy and feedstock; and to study the achievable economy by implementing new technologies and/or processes [13]. The exergetic analysis has been used for different MEE systems, such as for a triple-effect evaporator for concentrating orange juice [14]; a quadruple-effect [15] and a double-effect evaporator for the tomato paste industry [16]; a quintuple-effect evaporator in sugar industries [17]; and a complete milk power factory (including the evaporators) [18].

Researchers have developed studies that specifically consider exergy analysis in the pulp and paper industry. Gong [19] made a global exergy analysis of each step of the kraft process to produce cellulose. Cardoso et al. [20] developed models using industrial data to point out a suitable time for washing the evaporators, and to simulate the combustion in the recovery boiler in order to search for improvements. Utlu and Kincay [21] made a comprehensive energy and exergy analysis of a plant in which recycled wastepaper is used for papermaking. Mesfun and Toffolo [5] used process integration techniques from an energetic point of view to optimize a plant that considered three different integration boundaries: the MEE alone, the mill subprocess considered as a whole, and the total site. Diel et al. [22] used surface response methodology to optimize the MEE of the kraft process. Verma et al. [23] used Generic Algorithm in order to minimize the energy consumption in the MEE of the paper industry.

In some studies, the pulp and paper systems were described by considering all evaporators as a single black box [10,24]. When the evaporators were described individually, changes in the system configuration were proposed, but the influence of the values of the operational variables in process efficiency was not evaluated [25, 5, 11].

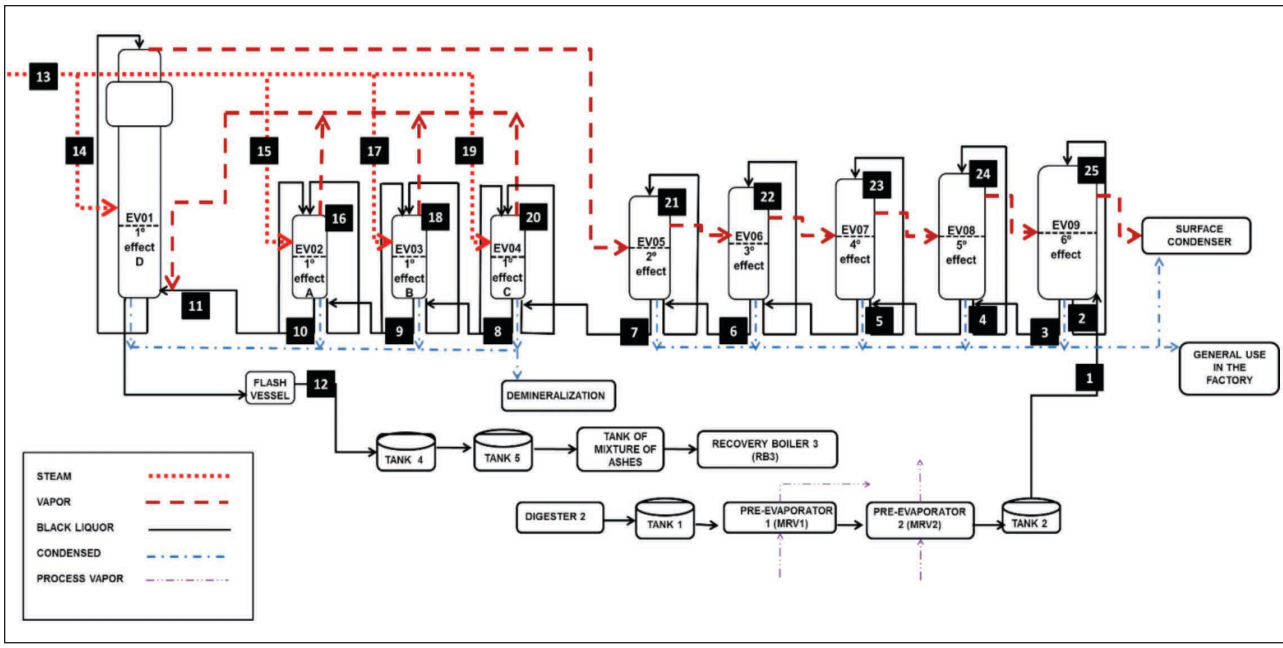

1. Multiple effect evaporator.

In the present work, each evaporator of a real kraft system is described individually using mass balance and thermodynamics principles (the first and the second laws). The global heat transfer coefficients $(UA)_i$ of the first effect are estimated using a nonlinear optimization routine and industrial data. The energetic and exergetic analysis of each evaporator of the MEE are presented. In addition to the energetic and exergetic analysis, a sensibility analysis of the system was made. Then, changes in the values of the operational variables were considered, in order to reproduce possible real conditions of the MEE, and the influence of these new operational conditions in the exergetic analysis was analyzed.

METHODOLOGY

System description

The considered system was the multiple effect evaporator (MEE) of a real kraft process in Minas Gerais, Brazil. In this plant, approximately 1.2 million metric tons of white cellulose are produced annually from short eucalyptus fiber. The system consists of nine evaporators distributed in six falling film effects, one surface condenser, and two pre-evaporators. **Figure 1** shows a simplified scheme of the MEE considered in the present work. The numbered collect points shown in Fig. 1 are detailed in **Table I**. The liquor in evaporators 1A, 1B, 1C and 1D has a concentration higher than 45%, which causes significant soiling in the equipment and creates the need for cleaning cycles. Therefore, evaporators 1A, 1B, 1C, and 1D work in alternate cycles, in which three of them work normally while the other is cleaned. Considering an operating cycle of 26 h, evaporator 1D is washed once and evaporators 1A, 1B, and 1C are washed twice. The 1D evaporator wash time is 2 h. Evaporators 1A, 1B, and 1C are washed for a period of 4 h. This work considers the operation while evaporator 1C is being cleaned.

Weak black liquor from the digester with approximately 16 %m/m solid concentration is pumped into storage tank 1. The liquor passes through two pre-evaporators (MVR; mechanic vapor recompression) connected in series and follows to storage tank 2 with about 19% solids concentration. It is then fed into the sixth effect, and passes through effects 5, 4, 3, 2, 1B, 1A, and finally 1D, having its solid concentration increase in each effect by water evaporation and achieving approximately 71 %m/m solids concentration. After effect 1D, the strong black liquor leaves the MEE and follows to the strong liquor tanks.

Low-pressure steam from the boiler feeds evaporators 1A, 1B, and 1D, where heat is transferred to the liquor and condensed water leaves each evaporator. Vapor from the black liquor in effects 1A and 1B are fed into effect 1D along with the liquor to increase turbulence, improving the heat exchange. Vapor from effect 1D is fed into effect 2 to transfer heat to the liquor. From effect 2 onward, the vapor from each effect is fed into the next one, in order to heat the liquor and evaporate water, and condensed water is collected from each effect. The condensates are classified according to the presence or absence of contaminants: the condensate extracted from effect 1 is called primary condensate; the condensate extracted from effects 2-6 is the secondary condensate; and the condensate from the surface condenser, which originates from the vapor of the sixth effect, is called tertiary condensate.

Operational data obtainment and treatment

The operational data used in this work correspond to measurements evaluated every 5 min from July 15 at 0:00 to July 19 at 23:00, in 2017, totaling 61447 measurements. Several data collected during that time describe the dynamic behavior of the system, and they were removed. During the analyzed period, evaporator 1C was cleaned several times and the data

Effect	Meaning	Unit	Collection Point*	Average	Standard Deviation	Maximum	Minimum
1	Total steam temperature	K	13	427.7	0.6	429.7	425.4
	Total steam pressure	kPa	13	392	10	412	373
	Total steam mass flow	$kg \cdot s^{-1}$	13	21.9	0.6	24.2	20.6
1D	Black liquor input concentration	% m/m	11	64.9	2.1	70.2	54.6
	Black liquor input density	$kg \cdot m^{-3}$	11	1300	30	1400	1200
	Black liquor input volume flow	$m^3 \cdot s^{-1}$	11	0.0383	0.0038	0.048	0.029
	Black liquor output concentration (flash vessel)	% m/m	12	71.0	1.4	73.7	57.8
	Black liquor output vol. flow (flash vassel)	$m^3 \cdot s^{-1}$	12	0.033	0.004	0.040	0.020
	Black liquor output temperature (flash vassel)	K	12	380.7**	unavailable	unavailable	unavailable
	Steam mass flow	$kg \cdot s^{-1}$	14	4.86	0.75	5.97	1.92
1A	Black liquor output temperature	K	10	413.7	1.0	415.6	411.0
	Vapor temperature	K	16	412.6	0.8	413.8	408.9
	Vapor pressure / operating pressure	kPa	16	160	9	170	130
1B	Black liquor output temperature	K	9	411.5	1.0	413.9	406.5
	Vapor temperature	K	18	412.6	0.8	413.8	408.9
	Vapor pressure / operating pressure	kPa	18	160	13	180	140
2	Black liquor output mass flow	$m^3 \cdot s^{-1}$	7	0.054	0.002	0.060	0.043
	Black liquor output concentration	% m/m	7	42.0**	unavailable	unavailable	unavailable
	Black liquor output temperature	K	7	391.3	0.5	393.8	388.9
	Vapor temperature	K	21	390.7	0.8	393.0	389.2
	Vapor pressure / operating pressure	kPa	21	100.4	2.4	107.6	91.7
3	Black liquor output temperature	K	6	369.2	0.2	369.4	366.6
	Vapor temperature	K	22	368.3	0.1	368.4	368.2
	Vapor pressure / operating pressure	kPa	22	79.2	3.1	84.8	72.0
4	Black liquor input temperature	K	5	351.4	0.1	351.5	351.3
	Vapor temperature	K	23	354.5	0.4	354.8	353.2
	Vapor pressure / operating pressure	kPa	23	51.0	0.8	53.0	49.0
5	Black liquor input temperature	K	4	338.3	0.5	340.0	337.9
	Vapor temperature	K	24	342.5	0.1	344.0	342.5
	Vapor pressure / operating pressure	kPa	24	36.3	0.6	38.6	35.1
6	Black liquor input density	$kg \cdot m^{-3}$	1	1056**	unavailable	unavailable	unavailable
	Black liquor input concentration	% m/m	1	15.6**	unavailable	unavailable	unavailable
	Black liquor input temperature	K	2	343.2	0.5	344.6	342.5
	Black liquor input mass flow	$m^3 \cdot s^{-1}$	1	0.155**	unavailable	unavailable	unavailable
	Vapor temperature	K	25	329.0	0.5	330.3	328.7
	Vapor pressure / operating pressure	kPa	25	31.4	0.6	33.2	30.4
	Black liquor output mass flow	$m^3 \cdot s^{-1}$	3	0.124**	unavailable	unavailable	unavailable

*Shown in Fig. 1.
** Values reported by factory operators.

I. Operational data for the multiple effect evaporator shown in Fig. 1.

Reference	Equation	Eq.
Chase & Nist-Janaf [26]	$Cp_W(T) = -203.606 + 1.52329 \cdot T - 3.196413 \cdot 10^{-3} \cdot T^2 + 2.474455 \cdot 10^{-6} \cdot T^3 + 3.855326 \cdot 10^{6} \cdot T^{-2}$	(1)
Smith et al. [27]	$Cp_V(T) = R \cdot M_W^{-1} \cdot (3.470 + 1.45 \cdot 10^{-3} \cdot T + 1.21 \cdot 10^{4} \cdot T^{-2})$	(2)
Frederick [28]	$Cp_L(T,x) = (1-x) \cdot Cp_W + x \cdot (463.02 + 4.47 \cdot T) + (12851.35 - 29 \cdot T) \cdot (1-x) \cdot x^{3,2}$	(3)
Hyland and Wexler [29]	$p^*(T) = \exp[-5.880 \cdot 10^{3} \cdot T^{-1} + 1.391 - 4.864 \cdot 10^{-2} \cdot T + 4.176 \cdot 10^{-5} \cdot T^2 - 1.445 \cdot 10^{-8} \cdot T^3 + 6.546 \cdot \ln(T)]$	(4)
Costa et al. [30]	$BPE(x) = 1.517e^{2,708 \cdot x}$	(5)
-	$T_L(T_V, x) = T_V + BPE$	(6)
Avelar et al. [31]	$\rho_L(\rho_W, T, x) = 0.387528 + \rho_W \cdot \{0.872307 + [x \cdot (0.216726 - 0.00246 \cdot T)]\}^{3,604995}$	(7)
Smith et al. [27]	$\lambda(T) = R \cdot M_W^{-1} \cdot \left[40660 + \int_T^{373.15\,K} (Cp_W - Cp_V)\, dT\right]$	(8)
-	$h_W(T) = \int_{T_R}^{T} Cp_W\, dT$	(9)
-	$h_V(T) = \int_{T_R}^{T} Cp_W\, dT + \lambda(T)$	(10)
-	$h_L(T,x) = \int_{T_R}^{T} Cp_L\, dT$	(11)
-	$s_W(T) = \int_{T_R}^{T} (Cp_W/T)\, dT$	(12)
-	$s_V(T) = -0.0113 \cdot T + 11.5908$	(13)
-	$s_L(T,x) = \int_{T_R}^{T} (Cp_L/T)\, dT$	(14)
-	$ex = h - h_0 - T_0 \cdot (s - s_0)$	(15)

II. Property and auxiliary equations of the mathematical model.

that describe this operational condition were also removed. These two situations promoted an important reduction of the number of measurements. Also, some outliers were excluded from the data sample in order to minimize possible measurement errors that may have occurred. After the data treatment, 47647 measurements were removed, and the remaining 13800 are characterized in Table I.

Modeling and simulation

The system considered in the mathematical modeling includes eight evaporators: 1D, 1A, 1B, 2, 3, 4, 5, and 6, which will be treated as evaporators 1-8, respectively. The following considerations were made:

- The system is in steady-state.
- Each phase in the evaporators are in perfect mixture.
- Only water is evaporated from the black liquor, and both liquor and vapor are in thermodynamic equilibrium.
- Ambient heat loss is neglected.
- The steam from the boiler, the vapor from the evaporators, and the condensed water are saturated.
- Each vapor leaves its effect at the operational pressure of its evaporator.
- The reference temperature (TR) is 273.15 K.
- The surrounding temperature (T0) is 298.15 K.

Input Variable	Value	Input Variable	Value
p_1	160 kPa	p_7	36 kPa
p_2	160 kPa	p_8	31 kPa
p_3	160 kPa	T_S	427.65 K
p_4	100 kPa	T_{L9}	343.15 K
p_5	79 kPa	$\dot{m}_{L2}$	49.09 kg·s^{-1}
p_6	51 kPa	x_2	0.6487 kg·kg^{-1}

III. Input variables of the mathematical model.

The thermodynamic property equations and the auxiliary equations used in this work are summarized in **Table II**.

The following process variables are considered to be known in order to solve the mathematical model: the operational pressure of each evaporator ($p_{1\text{-}8}$), the steam temperature (T_S), the temperature of the liquor entering evaporator 8 (T_{L9}), and the liquor mass flow rate and concentration leaving evaporator 2 ($\dot{m}L_2$, x_2). The data of the liquor from evaporator 2 were chosen as input variables because there was more data available, and it was more consistent and stable than the data of the liquor entering evaporator 8. **Table III** shows the values considered for each input variable in the mathematical model.

The temperature of the vapor leaving each evaporator is calculated by solving Eq. 4 for each given pressure, and the liquor temperatures depend on the boiling point elevation (BPE) (Eqs. 5-6). The calculated vapor temperatures are close to the experimental temperatures reported by industry operators.

The mass and energy balances used in this work exist in a steady-state process. The mass balance for the liquor/vapor phase is made for each evaporator, as shown in Eqs. 16-17:

$$\dot{m}_{L1} + \dot{m}_{V1} = \dot{m}_{L2} + \dot{m}_{V2} + \dot{m}_{V3} \tag{16}$$

$$for\ i = 2 - 8: \qquad \dot{m}_{L(i)} + \dot{m}_{V(i)} = \dot{m}_{L(i+1)} \tag{17}$$

where $\dot{m}_L$ is the liquor mass flow rate, $\dot{m}_V$ is the vapor mass flow rate, and the numbers 1-8 correspond to the flows leaving the respective evaporators. Number 9 corresponds to the liquor entering the process through evaporator 8. The balance of solids for each evaporator is shown in Eq. 18:

$$for\ i = 1 - 8: \qquad \dot{m}_{L(i)} \cdot x_i = \dot{m}_{L(i+1)} \cdot x_{(i+1)} \tag{18}$$

where x is the concentration of solids in the liquor. The global energy balance for each evaporator is shown in Eqs. 19-22.

$$\dot{m}_{L1} \cdot h_{L1} + \dot{m}_{V1} \cdot h_{V1} = \dot{m}_{L2} \cdot h_{L2} + \dot{m}_{V2} \cdot h_{V2} + \dot{m}_{V3} \cdot h_{V3} + \dot{m}_{S1} \cdot \lambda(T_S \tag{19}$$

$$for\ i = 2 - 3: \ \dot{m}_{L(i)} \cdot h_{L(i)} + \dot{m}_{V(i)} \cdot h_{V(i)} = \dot{m}_{L(i+1)} \cdot h_{L(i+1)} + \dot{m}_{S(i)} \cdot \lambda(T_S) \tag{20}$$

$$\dot{m}_{L4} \cdot h_{L4} + \dot{m}_{V4} \cdot h_{V4} = \dot{m}_{L5} \cdot h_{L5} + \dot{m}_{V1} \cdot \lambda(T_{V1}) \tag{21}$$

$$for\ i = 5 - 8:$$

$$\dot{m}_{L(i)} \cdot h_{L(i)} + \dot{m}_{V(i)} \cdot h_{V(i)} = \dot{m}_{L(i+1)} \cdot h_{L(i+1)} + \dot{m}_{V(i-1)} \cdot \lambda\left[T_{V(i-1)}\right] \tag{22}$$

where h_L is the liquor enthalpy, h_V is the vapor enthalpy, $\dot{m}_{Si}$ is the steam mass flow rate entering evaporator i, $\lambda(T)$ is the water latent heat of vaporization at temperature T, and T_S is the steam temperature.

To calculate the steam flows to evaporators 1, 2, and 3, heat transfer equations are added to the model (Eq. 23) [22]:

$$for\ i = 1 - 3: \qquad (UA)_i \cdot \left(T_S - T_{L(i)}\right) = \dot{m}_{S(i)} \cdot \lambda(T_S) \tag{23}$$

where (UA)i is the product of the global heat transfer coefficient and the heat transfer superficial area of the evaporator i.

The mathematical model consists in 27 main algebraic equations (Eq. 16-23) and 27 variables, which are: $\dot{m}_{L1}$, $\dot{m}_{L3}$, $\dot{m}_{L4}$, $\dot{m}_{L5}$, $\dot{m}_{L6}$, $\dot{m}_{L7}$, $\dot{m}_{L8}$, $\dot{m}_{L9}$, x_1, x_3, x_4, x_5, x_6, x_7, x_8, x_9, $\dot{m}_{V1}$, $\dot{m}_{V2}$, $\dot{m}_{V3}$, $\dot{m}_{V4}$, $\dot{m}_{V5}$, $\dot{m}_{V6}$, $\dot{m}_{V7}$, $\dot{m}_{V8}$, $\dot{m}_{S1}$, $\dot{m}_{S2}$, and $\dot{m}_{S3}$. The model can be solved numerically, but it required the estimation of the heat transfer coefficients multiplied by the heat transfer superficial areas ($UA_{1\text{-}3}$).

Nonlinear optimization problem

The estimation of the parameters $(UA)_1$, $(UA)_2$, and $(UA)_3$ depends on many factors, such as flow conditions and equipment geometry, making them specific for each system. To estimate the heat transfer coefficients, a nonlinear optimization problem was developed and solved. The objective function (f_{min}) of this problem is the minimization of square errors of the model predictions in relation to experimental data, as shown in Eq. 24:

$$f_{min}(UA_1, UA_2, UA_3) = \left(\dot{m}_{S,sum}^{exp} - \dot{m}_{S,sum}^{mod}\right)^2 + \left(\dot{m}_{S1}^{exp} - \dot{m}_{S1}^{mod}\right)^2 + \left(\dot{m}_{L1}^{exp} - \dot{m}_{L1}^{mod}\right)^2 + \left(\dot{m}_{L4}^{exp} - \dot{m}_{L4}^{mod}\right)^2 + \left(\dot{m}_{L8}^{exp} - \dot{m}_{L8}^{mod}\right)^2 + \left(\dot{m}_{L9}^{exp} - \dot{m}_{L9}^{mod}\right)^2 + \left(x_1^{exp} - x_1^{mod}\right)^2 + \sum_{i=4}^{9}\left(x_i^{exp} - x_i^{mod}\right)^2 \quad (24)$$

where *exp* indicates experimental data, *mod* indicates values predicted by the model, and $\dot{m}_{S,sum}$ is the sum of the three steam mass flow rates. Typical literature values were chosen as initial guesses for the optimization. The optimization problem was solved using commercial software Matlab (MathWorks; Natick, MA, USA).

Energetic and exergetic analysis

To analyze the MEE energetically and exergetically, several indicative parameters were calculated. The energetic efficiency (η_{En}) is calculated in Eqs. 25-26:

$$\eta_{En,1} = (\dot{m} \cdot \lambda)_{V1} / [(\dot{m} \cdot \lambda)_{S1} + (\dot{m} \cdot \lambda)_{V2} + (\dot{m} \cdot \lambda)_{V3}] \quad (25)$$

$$for\ i = 2 - 8: \quad \eta_{En,i} = (\dot{m} \cdot \lambda)_{Vi} / (\dot{m} \cdot \lambda)_{Si\ or\ V(i-1)} \quad (26)$$

The energetic losses (*EnL*) show the energy fraction that is wasted in byproducts. It is calculated in Eq. 27:

$$for\ i = 1 - 8: \quad EnL = \dot{m}_{Ci} \cdot h_{Ci} \quad (27)$$

The exergetic efficiency (η_{Ex}) is calculated for each effect in Eq. 28:

$$for\ i = 1 - 8: \quad \eta_{Ex,i} = (\sum \dot{m} \cdot \mathrm{ex})_{i,out} / (\sum \dot{m} \cdot \mathrm{ex})_{i,in} \quad (28)$$

The exergetic losses show the exergy fraction that is wasted in byproducts. It is calculated in Eq. 29:

$$for\ i = 1 - 8: \quad ExL = \dot{m}_{Ci} \cdot ex_{Ci} \quad (29)$$

The irreversibilities (*I*) cause exergy destruction and are calculated in Eq. 30:

$$I_i = \left(\sum \dot{m} \cdot \mathrm{ex}\right)_{i,in} - \left(\sum \dot{m} \cdot \mathrm{ex}\right)_{i,out} \quad (30)$$

The gain output ratio (GOR) is also a measurement of the efficiency of an MEE. It is calculated by dividing the energy needed to evaporate the water in a single effect without energy recycle with the actual energy used in the process, as shown in Eq. 31:

$$GOR = \left\{\left(\dot{m}_{V,1} + \sum_{i=4}^{8} \dot{m}_{V,i}\right) \cdot \left[h_V(T_{V,avg}) - h_W(T_{L9})\right]\right\} / \left[\dot{m}_{S,sum} \cdot \lambda(T_S)\right] \quad (31)$$

where $T_{V,avg}$ is the average temperature of the vapors leaving the evaporator, and $h_V(T_{V,avg})$ is the enthalpy of the vapor at this average temperature.

Another efficiency measurement is the steam economy (*SE*), reported by Verma et al. [23]. This measurement represents how much kg vapor is generated per kg of steam, and is calculated as follows:

$$SE = \left(\dot{m}_{V,1} + \sum_{i=4}^{8} \dot{m}_{V,i}\right) / \dot{m}_{S,sum} \quad (32)$$

Sensibility analysis

Using the estimated values for $(UA)_1$, $(UA)_2$, and $(UA)_3$, the mathematical model was solved many times modifying key input variables in order to observe and analyze their effect on: exergetic efficiency (η_{Ex}), the concentration of strong black liquor leaving evaporator 1 (x_1), and the irreversibilities (*I*). In the sensibility analysis calculations, the reference case was considered the one with the input variables described in Table II, except for the $\dot{m}_{L2}$ and the x_2, which were substituted for the calculated values of $\dot{m}_{L9}$ and x_9, as the latter ones describe properties of the liquor entering the MEE. The variation range of each input variable was chosen considering physical constraints of the real process, which were:

- Concentration of black liquor entering evaporator 8 (x_9): from -10% to 10%.
- Mass flow rate of black liquor entering evaporator 8 ($\dot{m}_{L9}$): from -10% to 10%.
- Steam temperature (T_S): from -4.0% to 4.0%.

RESULTS AND DISCUSSION

Parameter estimation and process simulation

The optimization problem was solved and the estimated values of $(UA)_1$, $(UA)_2$, and $(UA)_3$ were $3.32 \cdot 10^5$, $6.77 \cdot 10^5$, and $6.52 \cdot 10^5$ W·K^{-1}, respectively. For these estimated parameters and the input parameters of Table III, the mathematical model was solved and the results are shown in **Table IV**. The generated vapor total mass flow rate was 113.76 kg·s^{-1}, and the condensate total mass flow rate was 123.61 kg·s^{-1}.

Figure 2 shows the experimental and predicted values for most of the liquor solid concentrations, liquor mass flow rates, and steam mass flow rates. The average relative error of the obtained values was only 5.2%, showing good agreement between the real industrial data and the model predictions.

Energetic and exergetic analysis

Table V shows the energetic (η_{En}) and exergetic efficiency (η_{Ex}), the energetic (*EnL*) and exergetic losses (*ExL*), and the irreversibilities (*I*) for each effect, which were calculated in Eqs. 25-29.

In general, the energetic analysis in literature is only made for the global system, as Gong [19] reported an energetic efficiency of 68%, for example. In this work, a calculation for each effect was made to observe which are the best and least efficient. The energetic efficiency of the effects varies from 84% to 98% (Table V), in which effects 1A, 5, and 6 are the most efficient (95.8%–98.4%) and effects 1D and 1B are the least efficient (84.9%). The energetic losses, on the other

Stream	$\dot{m}$, kg·s^{-1}	T, K	*BPE*, K	*x*, kg·kg^{-1}	P, kPa	H, kJ·kg^{-1}	*S*, kJ·kg^{-1}·K^{-1}	*ex*, kJ·kg^{-1}
Liquor 1	44.54	396.96	10.52	0.7150	160	360	1.085	39.3
Liquor 2	49.09	395.23	8.79	0.6487	160	369	1.117	39.6
Liquor 3	58.82	393.02	6.57	0.5414	160	382	1.159	40.1
Liquor 4	67.46	378.20	5.45	0.4721	100	345	1.068	30.2
Liquor 5	88.99	370.16	4.00	0.3579	79	336	1.050	26.1
Liquor 6	108.41	358.47	3.36	0.2938	51	304	0.968	19.3
Liquor 7	125.91	349.70	3.01	0.2529	36	278	0.898	14.6
Liquor 8	142.47	346.00	2.78	0.2235	31	269	0.873	12.9
Liquor 9	158.30	343.15	2.62	0.2012	-	262	0.852	11.6
Vapor 1	22.92	386.45	-	-	160	2704	7.224	554.5
Vapor 2	9.73	386.45	-	-	160	2704	7.224	554.5
Vapor 3	8.65	386.45	-	-	160	2704	7.224	554.5
Vapor 4	21.53	372.76	-	-	100	2678	7.379	482.5
Vapor 5	19.42	366.16	-	-	79	2665	7.453	447.8
Vapor 6	17.49	355.11	-	-	51	2644	7.578	389.7
Vapor 7	16.56	346.69	-	-	36	2629	7.673	345.5
Vapor 8	15.83	343.23	-	-	31	2622	7.712	327.3
Steam 1	4.79	427.65	-	-	392	2782	6.758	772.0
Steam 2	10.30	427.65	-	-	392	2782	6.758	772.0
Steam 3	10.60	427.65	-	-	392	2782	6.758	772.0
Cond. 1	4.79	427.65	-	-	-	652	1.891	93.2
Cond. 2	10.30	427.65	-	-	-	652	1.891	93.2
Cond. 3	10.60	427.65	-	-	-	652	1.891	93.2
Cond. 4	22.92	386.45	-	-	-	476	1.457	46.1
Cond. 5	21.53	372.76	-	-	-	418	1.304	33.7
Cond. 6	19.42	366.16	-	-	-	390	1.229	28.3
Cond. 7	17.49	355.11	-	-	-	344	1.100	20.3
Cond. 8	16.56	346.69	-	-	-	308	0.999	14.9

IV. Properties of process streams.

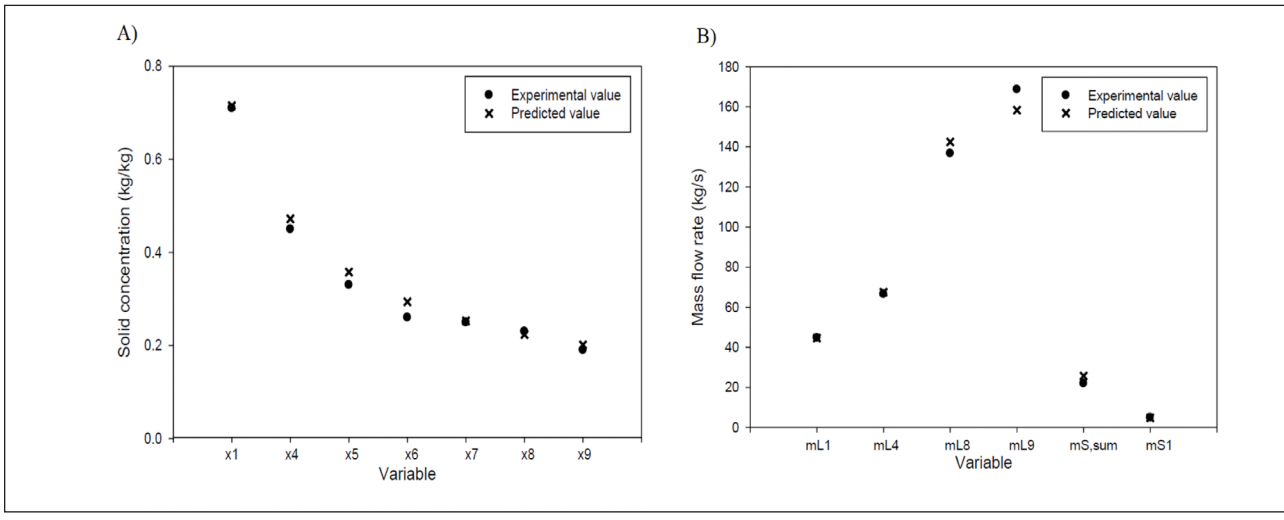

2. (A) Experimental and predicted values for liquor solid concentrations, and (B) liquor mass flow rates and steam mass flow rates.

Effect	η_{En}	η_{Ex}	*EnL*, kW	*ExL*, kW	*I*, kW
1D	0.849	0.942	3123.08	446.42	921.53
1A	0.984	0.805	6715.60	959.41	2010.93
1B	0.849	0.796	6911.20	987.98	2081.69
2	0.951	0.897	10909.92	1056.73	1555.83
3	0.908	0.941	8999.54	724.98	732.47
4	0.913	0.898	7573.80	549.68	1075.65
5	0.958	0.915	6016.56	354.30	735.25
6	0.963	0.961	5100.48	247.46	291.65

V. Energetic and exergetic parameters of each evaporator effect.

hand, show the highest loss for effects 2, 3, and 4 (7573–10909 kW), which have the greatest condensate mass flow rates, and the lowest loss for effect 1D (3123 kW), which has a low condensate mass flow rate.

The exergetic efficiency of the evaporator effects varies from 79% to 94% (Table V), in which effects 1D, 3, and 6 are the most efficient (94.1–96.3%) and have the least irreversibilities, and effects 1A and 1B are the least efficient (79.6%–80.5%) and have the highest irreversibilities. Macedo et al. [32] have also calculated the exergetic efficiency for each effect, but because a different equation was used, the results are not comparable. In their analysis, effect 8 was also the most exergetically efficient of all, showing agreement between the studies. The exergetic losses have a different tendency compared with the energetic losses. Effects 1A, 1B, and 2 have the highest *ExL* (959–1056 kW), because although effects 1A and 1B have low condensate mass flow rates, their specific exergy is higher than the condensates with lower temperature, compensating this difference in the overall analysis. Effect 8 has the lowest exergy losses (247 kW), as the condensate has the lowest temperature of all, meaning that its useful energy is low.

In the overall analysis, effects 1A and 1B are good candidates for optimization, as their exergetic efficiency is the lowest, meaning that they have more irreversibilities to be reduced in order to improve the overall process.

The GOR of the process is 5.00, which means that the energy necessary to concentrate the black liquor would be five times higher if there was no multiple effect system or energy recycle.

The SE of the process is 4.43, which means that 4.43 kg of water evaporates for each kg of steam demanded from the boiler. In the simulated model of Verma et al. (11), which consisted of a 7-effect evaporation system with a hybrid of steam-split, feed-split, and feed preheating process arrangements with backward feed flow, the optimum SE calculated by their model was 6.49, which is significantly higher than the one from a real plant in the present work. However, taking into account that in a real plant there are also some extra efficiency losses not considered in mathematical models, and that the plant considered in this work does not have extra strategies of feed splitting and feed preheating described by Verma et al. [11], the SE of the studied real plant is actually a reasonable value (although steam-split occurs between effects 1A, 1B, and 1D).

Sensibility analysis

The sensibility analysis of the mathematical model can be used to confirm an expected behavior and to investigate behavior that is not evident.

Figure 3 shows the simulated effect of varying liquor input concentration (x_9) on black liquor output concentration (x_1), irreversibilities (I), and exergetic efficiency (η_{Ex}). In Fig. 3A, it is observed that an increase of 10% in x_9 causes only a slight increase of 3% in x_1. In Fig. 3B and Fig. 3C, it is observed that no significant change occurs in the irreversibilities or in the η_{Ex} when x_9 is varied. Therefore, small variations of x_9 do not produce significant disturbances in the system.

Figure 4 shows the simulated effect of varying liquor input mass flow rate ($\dot{m}_{L9}$) on black liquor output concentration (x_1), irreversibilities (I), and exergetic efficiency (η_{Ex}). In Fig. 4A, it is observed that $\dot{m}_{L9}$ and x_1 have a significant linear relation. When the liquor flow rate is increased, more water has to be evaporated in order to achieve the same final concentration as in the previous situation, which explains the significant decreasing behavior of x_1 when $\dot{m}_{L9}$ is increased. Figures 4B and 4C shows that the irreversibilities and η_{Ex} are not significantly affected by a change in $\dot{m}_{L9}$, which may be explained by the fact that the nonuniformity (in this case the temperature difference between the steam and the liquor) remains constant. Therefore, the liquor input mass flow rate $\dot{m}_{L9}$ is a sensible parameter in the process that can be controlled with relative ease.

Figure 5 shows the simulated effect of varying steam temperature (T_S) on black liquor output concentration (x_1) (Fig. 5A), irreversibilities (I) (Fig. 3B), and exergetic efficiency

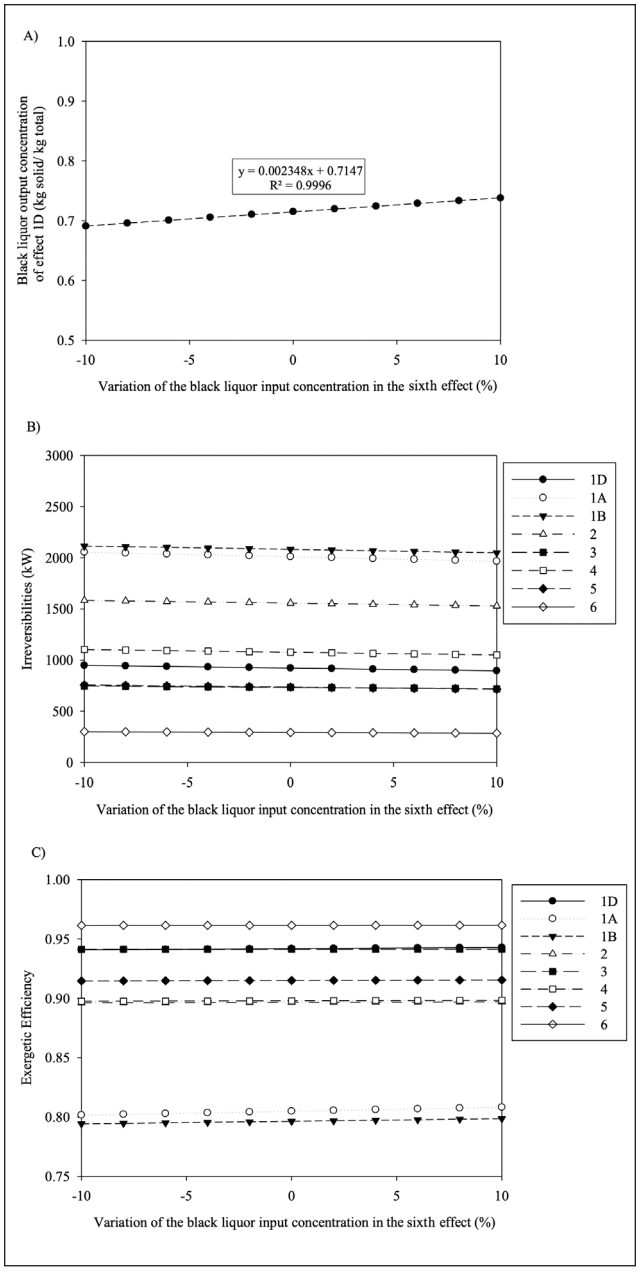

3. Effect of black liquor input concentration (x_9) on: (A) black liquor output concentration (x_1); (B) the irreversibilities of each effect (I); and (C) exergetic efficiency of each effect (η_{Ex}).

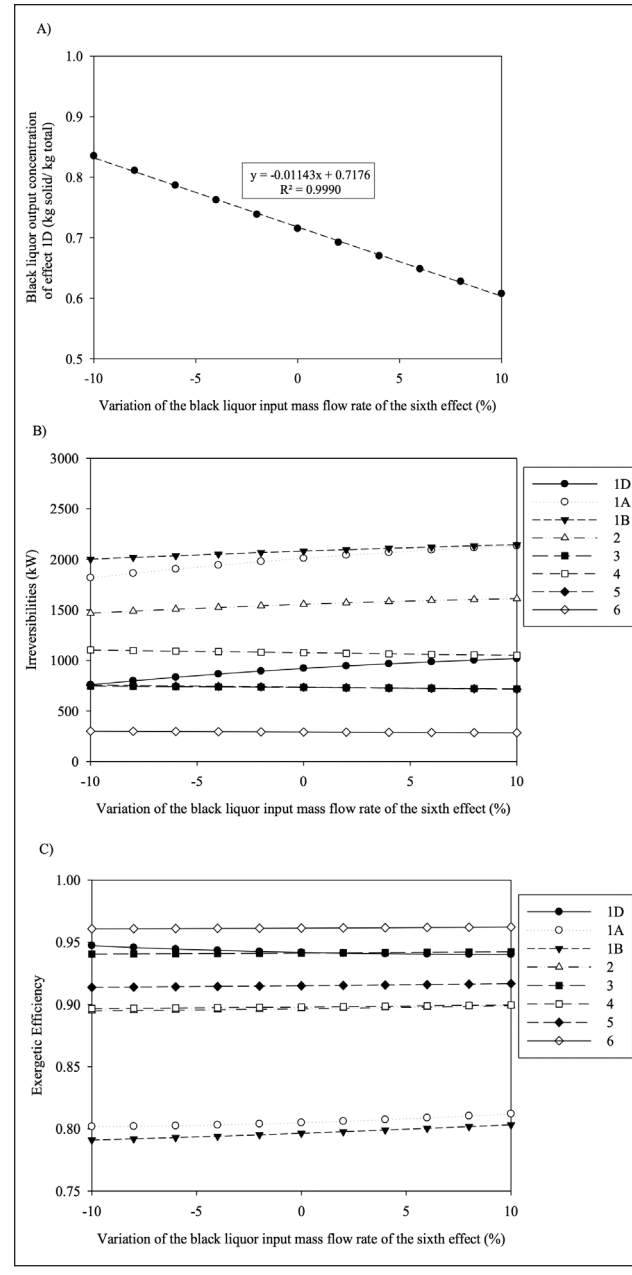

4. Effect of black liquor input mass flow rate ($\dot{m}_{L9}$) on: (A) black liquor output concentration (x_1); (B) the irreversibilities of each effect (I); and (C) exergetic efficiency of each effect (η_{Ex}).

(η_{Ex}) (Fig. 5C). In Fig. 5A, it is observed a significant linear relation exists between x_1 and T_S, so that a slight increase of 5°C could cause an increase of 10% in liquor concentration, and a decrease in T_S would decrease x_1 in a similar magnitude.

It is observed in Fig. 5B that the irreversibilities are increased with an increase in T_S. This effect is stronger in the first effects (1A and 1B), in which steam transfers heat to the liquor/vapor phase, and has little significance in the last ones. The nonuniformity of a system is proportional to the entropy generation by the power of two, and the irreversibilities are proportional to the entropy generation. In the process of the present work, the nonuniformity is caused by a temperature difference between the steam and the liquor, and it is enhanced when the steam temperature is increased. When T_S is increased, the nonuniformity, and, consequently, the irreversibilities are increased.

In Fig. 5C, it is observed that an increase in T_S causes a decrease in the exergetic efficiency of effects 1A and 1B, while no significant variation is observed in the other effects. This is in agreement with the irreversibilities results, as both of them depend on the exergy input and output (Eq. 28 and Eq. 30).

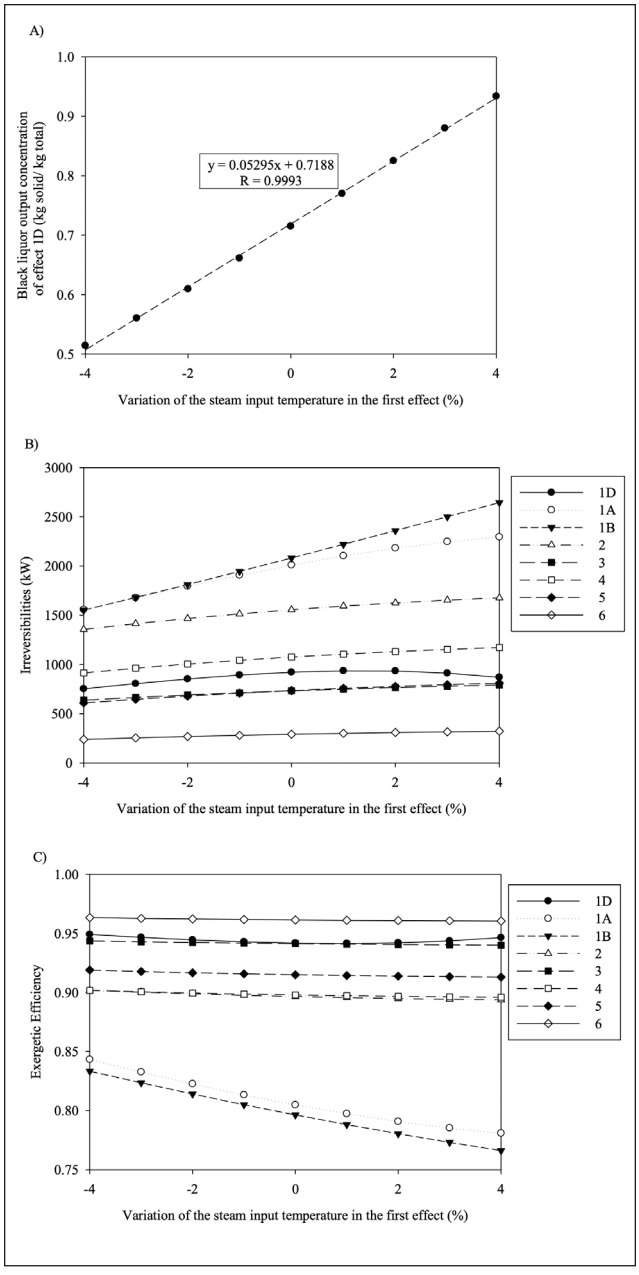

5. Effect of steam temperature (T_S) on: (A) black liquor output concentration (x_1); (B) the irreversibilities of each effect (I); and (C) exergetic efficiency of each effect (η_{Ex}).

Therefore, an increase in T_S leads to higher x_1, to higher irreversibilities, and to lower η_{Ex} in effects 1A and 1B. This increase in T_S could possibly increase the soiling rate as well, due to a higher liquor concentration in the first effect. Thus, steam temperature is a sensitive parameter and should be controlled with caution.

CONCLUSION

The methodology used in this study enabled detailed energetic and exergetic analysis of a real multiple effect evaporator (MEE) system. Each kraft evaporator was individually considered. For the mathematical description of the system, the heat transfer coefficients of the first effect were estimated using a nonlinear optimization problem and real industrial data. In similar studies, these parameters were typically obtained in the literature. However, the procedure used here can improve the obtained results, since these coefficients can be very specific for each system.

The developed mathematical model and the estimated parameters showed significant agreement with industrial data, as the average prediction error was only 5.2%.

The obtained results show that it is possible to determine which evaporators have the highest and lowest energy losses in the actual kraft pulp production process. Such information may assist mill personnel in the individual analysis of the operation of each piece of equipment, which is not always done in specialized literature.

The energetic analysis showed that effects 1D and 1B are the least efficient (84.9%) and effect 1A is the most efficient (98.4%). However, the more complete exergetic analysis showed that effects 1A and 1B are the least efficient (79.6% and 80.5%, respectively) and effect 6 is the most efficient (96.1%). The evaporators 1A and 1B have more potential for improvement, and should be the focus of optimization studies and proposals, in order to have a more efficient mill.

The sensibility analysis showed that steam temperature and the black liquor input mass flow rate are sensible input parameters to the system's efficiency and liquor output concentration. Therefore, they should be controlled with caution, in order to avoid oscillations, as deviations as small as 5°C could cause disturbances of about 10% in the liquor output concentrations and in the exergetic efficiency of effects 1A and 1B.

All results generated during this study were obtained considering time and operational condition specifics (when evaporator 1C is being cleaned, for example). To obtain a more detailed analysis, it is necessary to repeat the tests for each different cleaning cycle. The obtained results show that the proposed methodology can be expanded.

Finally, the authors affirm that is possible to adapt the presented model to propose an automatic mathematical routine that can be used to optimize the operational conditions of the process. All the information necessary to reproduce the obtained results are present in this article. Thus, mills engineers can adapt the presented equations to a different plant and propose a new tool to help the scheduled routine of the mill. **TJ**

ACKNOWLEDGEMENTS

The authors are grateful to CAPES and FAPEMIG (TEC-APQ-00914-16) for their financial support.

LITERATURE CITED

1. Ashrafi, O., Yerushalmi, L., and Haghighat, F., *J. Environ. Manage.* 158: 146(2015).
2. Costa, A.O.S., Biscaia Jr., E.C., and Lima, E.L., *Comput. Chem. Eng.* 28(5): 633(2004). https://doi.org/10.1016/j.compchemeng.2004.02.008.

3. Costa, A.O.S., Biscaia Jr., E.C., and Lima, E.L., *Can. J. Chem. Eng.* 83(3): 477(2005). https://doi.org/10.1002/cjce.5450830310.
4. Costa, A.O.S., Souza Jr., M.B., Biscaia Jr., E.C., et al., *TAPPI J.* 4(4): E33(2005).
5. Mesfun, S. and Toffolo, A., *Appl. Energy* 107: 98(2013). https://doi.org/10.1016/j.apenergy.2013.02.016.
6. Silva, W.L., Ribeiro, J.C.T., Costa Jr., E.F., et al., *Braz. J. Chem. Eng.* 25(3): 603(2008). https://doi.org/10.1590/S0104-66322008000300017.
7. Bajpai, P., *Management of Pulp and Paper Mill Waste*, Springer International Publishing, Cham, Switzerland, 2015, pp. 9-39.
8. Chantasiriwan, S., *Chem. Eng. Commun.* 204(12): 1466(2017). https://doi.org/10.1080/00986445.2017.1367674.
9. Costa, A.O.S. and Lima E.L., *Can. J. Chem. Eng.* 81(5): 1032(2003). https://doi.org/10.1002/cjce.5450810514.
10. Goortani, B.M., Mateos-Espejel, E., Moshkelani, M., et al., *Appl. Therm. Eng.* 31(17-18): 4091(2011). https://doi.org/10.1016/j.applthermaleng.2011.08.016.
11. Verma, O.P., Mohammed, T.H., Mangal, S., et al., *Energy* 129: 148-157(2017). https://doi.org/10.1016/j.energy.2017.04.093.
12. Mateos-Espejel, E., Savulescub, L., and Paris, J., *Chem. Eng. Res. Des.* 89(6): 742(2011). https://doi.org/10.1016/j.cherd.2010.09.012.
13. Wall, G., *Energy (Oxford)* 13(2): 197(1988). https://doi.org/10.1016/0360-5442(88)90046-1.
14. Balkan, F., Colak, N., and Hepbasli, A., *Int. J. Energy Res.* 29(5): 455 (2005). https://doi.org/10.1002/er.1074.
15. Sogut, Z., Ilten, N., and Oktay, Z., *Energy* 35(9): 3821(2010). https://doi.org/10.1016/j.energy.2010.05.035.

ABOUT THIS PAPER

Cite this article as:
Moreira, J., Campos, B., da Costa Junior, E., and da Costa, A., *TAPPI J.* 18(10): 605(2019).
https://doi.org/10.32964/TJ18.10.605

DOI: https://doi.org/10.32964/TJ18.10.605

ISSN: 0734-1415

Publisher: TAPPI Press

16. Soufyian, M.M., Dadak, A., Hosseini, S.S., et al., *Energy* 111: 910(2016). https://doi.org/10.1016/j.energy.2016.06.030.
17. Bapat, S.M., Majali, V.S., and Ravindranath, G., *Int. J. Energy Res.* 37(12): 1415(2013). https://doi.org/10.1002/er.2940.
18. Bühler, F., Nguyen, T.V., Jensen, J.K., et al., *Energy* 162: 576(2018). https://doi.org/10.1016/j.energy.2018.08.029.
19. Gong, M., *Int. J. Energy Res.* 29(1): 79(2005). https://doi.org/10.1002/er.1041.
20. Cardoso, M., Oliveira, K.D., Costa, G.A.A., et al., *Appl. Energy* 86(1): 45(2009). https://doi.org/10.1016/j.apenergy.2008.03.021.
21. Utlu, Z. and Kincay, O., *Energy* 57: 565(2013). https://doi.org/10.1016/j.energy.2013.05.054.

ABOUT THE AUTHORS

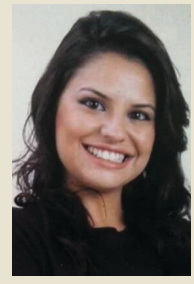
Moreira


Campos


da Costa Junior


da Costa

I (Andréa Oliveira Souza da Costa) have researched kraft process topics since 1996, including mathematical modeling of kraft evaporators, and this study is a continuation of those previous studies. Although we have used exergy analysis—an interesting thermodynamic tool—to analyze other industrial systems, this is the first time we have used it to describe kraft evaporator systems.

The most difficult aspect of this research was to validate the mathematical model of the process. For this, our master's student (Moreira) visited the mill and collected the industrial data. On my part, I helped my co-authors understand the thermodynamic aspects of the proposed methodology and also helped obtain the industrial data and financial support.

The most interesting aspect of this research was to confirm the adequacy of the proposed methodology to individually describe kraft evaporators, as in the literature, kraft evaporators are often described as a "black box."

Mill engineers can use the proposed mathematical model to describe their evaporator systems. Our next step is to propose an automatic routine to optimize kraft evaporators.

Moreira is a deployment analyst, Campos is a Ph.D. candidate in Chemical Engineering, and da Costa Junior and da Costa are professors in the Chemical Engineering Department, Universidade Federal de Minas Gerais (UFMG), Belo Horizonte, MG, Brazil. Email da Costa at andreaosc@yahoo.com.br.

22. Diel, C.L., Canevesi, R.L.S., Zempulski, D.A., et al., *Appl. Therm. Eng.* 95: 18(2016). https://doi.org/10.1016/j.applthermaleng.2015.10.136.
23. Verma, O.P., Manik, G., Suryakant, et al., *Sustainable Computing: Informatics and Systems* 20: 130(2018). https://doi.org/10.1016/j.suscom.2017.11.005.
24. Mateos-Espejel, E., Savulescu, L., Maréchal, F., et al., *Chem. Eng. Sci.* 66: 135(2011). https://doi.org/10.1016/j.ces.2010.09.032.
25. Bonhivers, J.C., Svensson, E., Sorin, M.V., et al., *Appl. Therm. Eng.* 75: 547(2015). https://doi.org/10.1016/j.applthermaleng.2014.09.045.
26. Chase, M.W. and Nist-Janaf, J.R., *J. Phys. Chem. Ref. Data, Monogr. 9,* 1998, pp. 1-1951.
27. Smith, J.M., Van Ness, H.C., and Abbott, M.M., *Introduction to Chemical Engineering Thermodynamics*, 7th edn., McGraw-Hill, New York, 2005.
28. Adams, T.N., Frederic, W.J., Grace, T.M., et al., *Kraft Recovery Boilers*, 1st edn., TAPPI Press, Peachtree Corners, GA, USA, 1997, p. 381.
29. Hyland, R.W. and Wexler, A., *ASHRAE Trans.* 89(2A): 500(1983).
30. Costa, A.O.S, Silva, S.C., Barañano, A.G., et al., *O Papel* 77(10): 88(2016).
31. Avelar, G.A., Oliveira, E.D., Park, S.W., et al., *Appita J.* 60(4): 321(2007).
32. Macedo, J.C.F., Reis, H.M., and Silva, R.J., Análise exergética de uma planta de evaporação de múltiplos efeitos do processo de extração de celulose pelo processo kraft," *Congresso e Exposição Internacional de Celulose e Papel* - ABTCP, 44, ABTCP, São Paulo, SP, Brazil, 2009.